

Learning to Arbitrate Human and Robot Control using Disagreement between Sub-Policies

Yoojin Oh¹, Marc Toussaint^{2,3} and Jim Mainprice^{1,3}

¹Machine Learning and Robotics Lab, University of Stuttgart, Germany

²Learning and Intelligent Systems Lab ; TU Berlin ; Berlin, Germany

³Max Planck Institute for Intelligent Systems ; MPI-IS ; Tübingen/Stuttgart, Germany

Abstract—In the context of teleoperation, arbitration refers to deciding how to blend between human and autonomous robot commands. We present a reinforcement learning solution that learns an optimal arbitration strategy that allocates more control authority to the human when the robot comes across a decision point in the task. A decision point is where the robot encounters multiple options (sub-policies), such as having multiple paths to get around an obstacle or deciding between two candidate goals. By expressing each directional sub-policy as a von Mises distribution, we identify the decision points by observing the modality of the mixture distribution. Our reward function reasons on this modality and prioritizes to match its learned policy to either the user or the robot accordingly. We report teleoperation experiments on reach-and-grasping objects using a robot manipulator arm with different simulated human controllers. Results indicate that our shared control agent outperforms direct control and improves the teleoperation performance among different users. Using our reward term enables flexible blending between human and robot commands while maintaining safe and accurate teleoperation.

I. INTRODUCTION

The level of autonomy in robot teleoperation, and hence shared control between the human and the robot, is a hot topic of both academic and industrial research & development. Shared autonomy is especially desirable when the environment is structured but the task objectives are unspecified and have to be decided in real-time, such as disaster relief [1], or autonomous driving [2], or the control of assistive devices, for instance, controlling a robotic arm using a cortical implant [3] or a robotic wheelchair, where the human control authority is a key feature [4].

Traditional approaches to robot teleoperation rely on the user assigning low-level (*direct control*) or mid-level (*traded control*) commands to be performed by the robot. In these cases, the human always has control over the robot's actions. In contrast, *shared control* arbitrates between human and robot control by inferring the human intent, and executing the action autonomously when possible. Shared control can mitigate difficulties linked to direct control, which originate from human bounded rationality, limited situation awareness and the discrepancy between the human and robot morphologies.

Shared autonomy systems rely on two components:

- 1) prediction of user intent
- 2) blending user vs. autonomous controls

Corresponding author: yoojin.oh@ipvs.uni-stuttgart.de

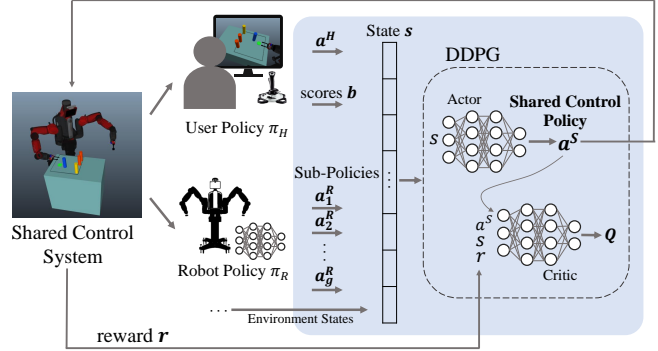


Fig. 1: Overview of our method using the DDPG (Deep Deterministic Policy Gradient) algorithm. The arbitration module takes as input the user policy, the sub-policies for all goals, their scores, and outputs a continuous arbitrated policy.

Trading off robot and human control is usually directly based on the confidence scores associated with the intent prediction module. This paper focuses on the blending strategy (i.e., arbitration), and leaves the prediction to other works.

Our approach (see Figure 1) learns an arbitration strategy from user interaction. This is generally beneficial as different users may have different preferences. Though tempting, it is difficult to learn an arbitration function using supervised learning. Indeed the introduction of the arbitration will inevitably shift the data distribution and hence the behavior of the human in return.

Several works have studied the problem of using reinforcement learning in shared control. However, to the best of our knowledge, no work has focused on learning directly the arbitration module while leveraging the local geometry of the available sub-policies. This is desirable to limit the sample complexity by 1) limiting the search space by using readily available optimal actions, 2) making use of the disagreement between the sub-policies and the shared actions to create implicit feedback, resulting in dense rewards.

Finally, to solve continuous action spaces control tasks common in robotic applications, we apply the modern actor-critic algorithm Deep Deterministic Policy Gradient (DDPG) [5].

We summarize our main contributions as the following:

- A generic arbitration learning formulation, which we cast as an actor-critic reinforcement learning problem

- Identification of “decision points” in the environment, where the robot encounters multiple options
- A new reward term that allows to maximize human control authority near decision points, by implicit feedback in continuous domains
- Quantitative results in simulation that show the effectiveness of the approach on a realistic robot manipulation scenario.

This paper is structured as follows: We first go over related work in Section II, we then present our method in Section III. We introduce our framework and explain the implementation in Section IV, and results are discussed in Section V. Finally, conclusions are drawn in Section VI.

II. RELATED WORK

A. Arbitration in Shared Control

One common form of blending is through a linear combination between the human user and autonomous robot agent policies [6], [7], [8], [9]. Generally the arbitration function $\alpha : (a^H, a^R) \mapsto a^S$, given user and robot actions a^H, a^R and outputs an arbitrated action a^S , can depend on different factors such as the confidence in the user intent prediction [6], [9], [8], or considering the difference between each commands [7].

When the robot predicts the user’s intent with high confidence, the user often loses *control authority*. This has been reported to generate mixed preferences from users where some users prefer to keep control authority despite longer completion times [10], [11]. Additionally, when assistance is against the user’s intentions this approach can aggravate the user’s workload [6]; the user “fights” against the assistance rather than gain help from it. Defining an arbitration function that is not too *timid* (i.e., only gives assistance when very confident) nor to *aggressive*, is generally difficult and interpreting the noisy confidence estimate of the intent prediction is prone to errors.

Some works have taken the option to allocate maximum control authority to the user by minimally applying assistance only when it is necessary. Broad et. al. [12], [13] introduced minimum intervention shared control that computes whether the control signal leads to an unsafe state and replaces the user control if so. However, these works usually model the problem by selecting an action within a feasibility set. Here we tackle problems with continuous action where such a set is difficult to characterize.

To alleviate this issue we have proposed “Natural gradient shared control” [14], where we formulate shared control as an optimization problem. The shared action is chosen to maximize the user’s internal action-value function while constraining the shared control policy to not diverge away from the autonomous robot policy. This approach is based on the availability of a global goal-conditioned optimal policy for the robot. This is nowadays only available for low-dimensional domains with perfect state estimation, however it is anticipated that with the advances of reinforcement learning [15], [16], such control policies should become

available for an increasing number of domains. However, despite this formulation of the problem, it is desirable to tune the arbitration online so as to account for user preferences.

B. Reinforcement Learning for Shared Control

Recent works have proposed to use reinforcement learning for shared control (RLSC) in different application contexts. In [17], SARSA, an on-policy reinforcement learning algorithm, is used to produce an arbitration weight for a walking-aid robot. The reward function penalizes collision with environment and promotes smoothness. In contrast to our work, no *implicit feedback* from the user is considered.

The notion of implicit feedback as a reward term is introduced in [18] to train an agent for a X-to-Text application. The error correction input (i.e., backspace) from the user is used to penalize the wrong actions taken by the autonomous agent.

In recent years, some model-free RLSC methods have been proposed. The earliest work is [19], where the agent maximizes a combination of task performance and user feedback rewards using Deep-Q learning. In [20], the approach is extended to maximize human-control authority using residual policy learning. While general, model-free approaches do not consider the structure of the problem to maximize adaptability at the cost of sample complexity. Instead, our approach investigates the case where robot sub-policies are available. In our experiments, these correspond to goal-conditioned policies, but they do not have to be.

In [21], Fernandez and Caarls develop an RLSC agent to learn a haptic policy using a type of implicit feedback, which compares the velocity the user applies with the forces exerted. While similar to our approach, their approach does not make use of an available optimal policy, which is instead learned online.

The ideas developed in RLSC have been generalized in [22], which formalizes a framework for assistive systems where the notion of human *empowerment* is introduced to denote reward terms that promote the user control over the state. The reward function we propose can be viewed as a type of empowerment proxy, especially designed to account for sub-policies in continuous action spaces, which are common in robot control problems.

III. REINFORCEMENT LEARNING FOR ARBITRATION

A. Problem Setting

In shared control where a human agent and the robot agent shares control to accomplish a mutual task, the state space includes the user action $a^H \in \mathcal{A}^H$, the robot actions $a_g^R \in \mathcal{A}_g^R$ for each goal $g \in \mathcal{G}$. Each robot action a_g^R may result from a different sub-policy indexed by g , in our experiments we simply conditioned a single policy on g . Each goal or sub-policy is associated with a confidence score or belief b_g . The shared control agent produces an arbitrated action $a^S \in \mathcal{A}^S$.

B. Learning an Arbitrated Policy

A reinforcement learning agent for arbitration strategy, learns a policy $\mu(a_t^S|x_t)$, which takes as input

$$s_t = \{x, a^H, a_1^R, \dots, a_g^R, b_1, \dots, b_g\}$$

where x is the environment states (e.g. gripper position, distance to goals, distance to obstacle). Our reinforcement learning problem is modeled as an optimal control task of a Markov Decision Process (MDP), which is defined by a set of states \mathcal{S} , a set of actions \mathcal{A} , transition probabilities $\mathcal{T} : \mathcal{S} \times \mathcal{A} \times \mathcal{S}$, a reward function $\mathcal{R} : \mathcal{S} \times \mathcal{A} \rightarrow \mathbb{R}$, and a discount factor $\gamma \in [0, 1]$.

To devise the arbitration strategy μ , we follow the DDPG algorithm [5], but we point out two adjustments that distinguish our method from the standard version, both are reported in Algorithm 1.

a) Sub-policies: We utilize all sub-policies when considering the arbitration rather than one policy. At each time step of the episode, we query all possible sub-policies towards each object and compute the scores.

In our experiments, the sub-policies $a_{t,g}^R$ represent the action for each prospective goal object g and details of the sub-policies are later explained in Section IV-B. The score b_g denotes how likely the object is the goal and it can be described as the posterior probability given a history of observed features $\xi_{S \rightarrow U}$ [6], [23]. The predicted goal object g^* naturally becomes the object with the highest score. However, we do not emphasize one goal when learning the arbitrated action. We let the network take into account the inaccuracy of the intent prediction.

b) Hindsight goal labeling: Since we do not explicitly provide the true goal g^* that the user is intending, we store the state-action pairs in a separate episode buffer R_E and compute the rewards for each state-action pair in hindsight once the episode terminates. The off-policy characteristic of the DDPG algorithm enables us to update the replay buffer R in a delayed manner, as it already randomly samples a minibatch from R to update the parameters of the network. We first collect n episodes to fill the replay buffer to compensate the delayed population of R .

We propose an arbitration strategy that allocates more control authority when the robot needs to decide. Rather than making imperfect intent predictions to decide on which goal or direction to assist towards, we actively let the user decide instead. These decision points are identified by observing how the sub-policies diverge and creating implicit feedback in the form of a specific reward term.

C. Identifying Decision Points

A decision point is where one has to choose an option given multiple options. A robot agent may encounter them explicitly through intersections or getting around obstacles, or implicitly such as deciding to choose a goal given multiple prospective goals.. In a human-robot collaboration task such as teleoperation, inferring the user intent or the goal can mitigate this problem by estimating the belief over the

Algorithm 1: DDPG for Arbitration Learning

Init:

Load actor $\mu(s|\theta^\mu)$, critic $Q(s, a|\theta^Q)$ weights θ^μ, θ^Q
Initialize target network μ', Q' with weights
 $\theta^{\mu'} \leftarrow \theta^\mu, \theta^{Q'} \leftarrow \theta^Q$

Initialize replay buffer R , episode buffer R_E

for episode = 1, M **do**

for $t = 1, T$ **do**

 Observe user action a_t^H

foreach $g \in \mathcal{G}$ **do**

 Query sub-policy action $a_{t,g}^R$

 Compute score $b_{t,g}$

 Select action $a_t^S = \mu(s_t|\theta^\mu) + \mathcal{N}_t$

 Execute a_t^S , observe next state s_{t+1} , done d_t

 Store transition $(s_t, a_t^S, s_{t+1}, d_t)$ in R_E

if $t > n$ **then**

 Sample a random minibatch of N

 transitions $(s_i, a_i, r_i, s_{i+1}, d_t)$ from R

 Update $\theta^\mu, \theta^{\mu'}, \theta^Q, \theta^{Q'}$

 Observe true goal g^*

foreach $o \in R_E$ **do**

 Compute reward $r_i = \text{Reward}(o, g^*)$

 Store transition $(s_i, a_i^S, r_i, s_{i+1}, d_t)$ in R

possible goals. However, the intent may only be more certain once the robot has passed the decision point.

Our approach lets the user take more control when there is a decision point in the environment. In a problem setting with a discrete number of goals, we identify a decision point by looking at how the sub-policies for the goals are distributed. When the robot encounters an obstacle, the sub-policies show two divergent paths that the robot can take. Similarly, when the robot is between two goal objects, the policies for each object will result in two divergent paths that the robot can take. Rather than relying on an intent prediction method, we explicitly allocate more control authority to prevent the robot from assisting towards the wrong goal.

We express each sub-policy towards a goal as a conditional probability distribution $\pi(a|s, g)$ of taking an action a at state s for a goal g .

$$\pi(a|s) = \sum_{g \in \mathcal{G}} \pi(a|s, g)p(g) \quad (1)$$

The marginalized probability $\pi(a|s)$ is a mixture model which is a weighted sum over the conditional probabilities $\pi(a|s, g)$ with probability $p(g)$, for a discrete set of goals $g \in \mathcal{G}$. The decision points are identified by reasoning on the modality of the distribution $\pi(a|s)$. A single mode corresponds to having no decision point, while multiple modes indicate a decision point.

D. Directional Policies on the Plane

Consider a 1-dimensional action case, where the action is an angle. Each sub-policy $\pi(a|s, g)$ can be modeled as a von Mises distribution, as shown in Figure 2. Von Mises distributions express a probability distribution along all *directions* in the plane, which is a continuous distribution

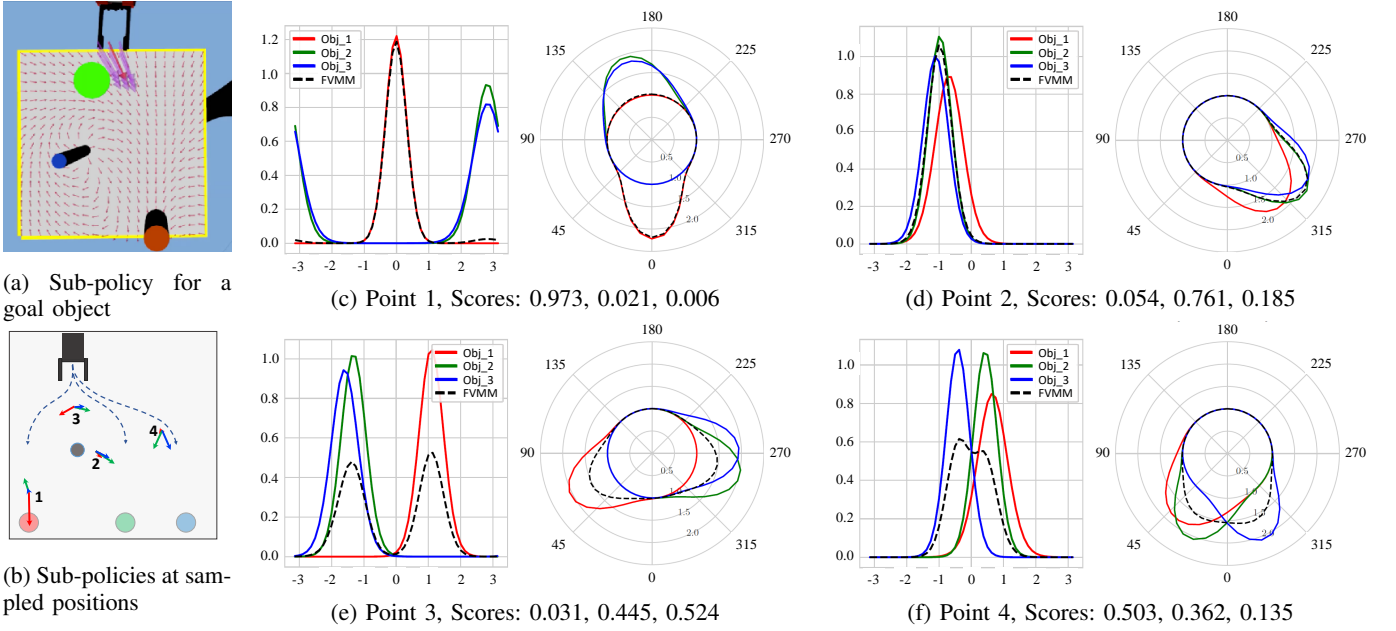


Fig. 2: Von Mises distributions for each sub-policy (solid colored line, matching the colors of the objects in (b)) and its Finite von Mises Mixture Model (FVMM) (black dashed line). Top row: Conditions when the robot should take control, clear intention towards an object (c), similar sub-policies (d). Bottom row: Conditions when the human should take control, deciding which direction to get around the obstacle (e), in between two perspective goal objects (f).

on a unit circle [24]. The general von Mises probability density function is expressed as:

$$f(x|\mu, \kappa) = \frac{1}{2\pi I_0(\kappa)} \exp^{\kappa \cos(x-\mu)} \quad (2)$$

where the parameters mode μ and dispersion $1/\kappa$ are comparable to the mean μ and the variance σ^2 in the normal distribution, and $I_0(\kappa)$ is the modified Bessel function of order 0. In higher dimensions, it takes the form of a von Mises-Fisher distribution over a n-sphere.

For each sub-policy, the mode μ of the distribution shows the direction of the action with the highest probability and the dispersion κ is related to the scores from the goal prediction.

The resulting $\pi(a|s)$ is a Finite von Mises Mixture model (FVMM). When the robot is near an obstacle or approaching to grab an object (situations where robot assistance is needed), all sub-policies are similar (co-directed) or one sub-policy dominates others (points 1 & 2 in Figure 2b). The mixture distribution $\pi(a|s)$ is unimodal, as shown in Figures 2c, 2d, and indicates the condition where the robot should take more control authority.

When the robot is near a decision point, e.g. approaching an obstacle or in between two goal objects (points 3 & 4 in Figure 2b), the sub-policies disagree. The resulting mixture distribution becomes multimodal with modes in the possible directions that the robot can take, as shown in Figures 2e, 2f. Here, we allocate more control authority to the user.

E. Reward Function using Disagreement

The overall algorithm for computing the reward is summarized in Algorithm 2. The reward function consists of a reward term based on the agreement of the policies

Algorithm 2: Reward Function

Input: s_t, a_t^S, g^*

Output: r_t

Function Reward(s_t, a_t^S, g^*):

 Compute R_{env}

 Means $\mathcal{M} = \{a_{t,g}^R\}_{g=1}^G$

 Dispersions $\mathcal{K} = \{b_{t,g}\}_{g=1}^G$

 Construct FVMM

$$\pi(a_t|s_t) = \frac{1}{2\pi I_0(\kappa)} \exp^{\kappa \cos(a_t - \mu)}$$

if multimodal **then**

$$R_{agree} = -||a_t^H - a_t^S||^2$$

else

$$R_{agree} = -||a_{t,g^*}^R - a_t^S||^2$$

$$R_{speed} = -||a_t^H|| - ||a_t^S||$$

$$R_{agree} \leftarrow R_{agree} + R_{speed}$$

$$r_t \leftarrow R_{agree} + R_{env}$$

return r_t

End Function

R_{agree} and R_{env} to penalize or reward certain actions while interacting with the environment.

$$R(s, a, s') = R_{agree} + R_{env} \quad (3)$$

R_{env} includes negative reward when the robot is in collision with the obstacle (-10) or the workspace boundary (-2) and positive reward when the gripper reaches the goal object (+10). R_{agree} is provided as a form of implicit feedback, by penalizing the disagreement between agent policies depending on the modality of the FVMM. When it is multimodal, R_{agree} penalizes the L2 norm between the human agent a^H and the arbitrated action a^S . When the FVMM is unimodal,

R_{agree} penalizes the L2 norm between the robot action $a_{g^*}^R$ and the arbitrated action a^S . The actions are normalized prior to computing the L2 norm and $a_{g^*}^R$ indicates the sub-policy for the true goal g^* that the user intended, which is accessible in hindsight once the episode terminates. R_{agree} is additionally subtracted with the absolute difference between the norms of a_t^H and a_t^S (denoted as R_{speed}) to match the policy’s speed to that of the human’s.

There can be multiple ways to determine the modality of the FVMM. In the algorithm, we sample a number of points from the FVMM and examine whether a peak value exists that exceeds a threshold. When the FVMM is unimodal, there is one peak that exceeds the threshold due to its narrow dispersion. There are no peaks detected that exceeds the threshold when the FVMM is multimodal.

IV. EXPERIMENTAL SETUP

We provide experimental details on training the model and evaluate the performance of our shared control agent. We hypothesize the following:

- The shared control agent can learn to flexibly allocate more control authority to the human when the prediction is unclear and provide more assistance when the goal is clear.
- The custom reward function enables faster convergence when training and it enables safe and accurate execution towards the user’s intended goal.

A. Environment Details

We consider a teleoperation task where the human agent is controlling the end-effector of a robot manipulator to reach and grab the goal object while avoiding an obstacle. The simulated environment consists of a table with objects and a Baxter robot (see Figure 1). The robot can manipulate its end-effector on a parallel plane above the 50cm×50cm table workspace. Graspable objects are placed at the end of the workspace, and the obstacle is randomly located near the middle of the workspace. The gripper position is initialized to start behind the obstacle so that the robot arm encounters the obstacle when reaching for the goal object. Physical collisions are not included in the simulated environment.

B. Obtaining Robot Sub-policies

We train a goal-conditioned neural network policy π_g by imitating optimized robot grasping trajectories. We obtain multiple sub-policies by pre-conditioning the policy on different goals.

The state and action space of our robot policy is solely defined in task space. Consequently, the network must learn to output end-effector actions that avoid collision with the whole arm. We collect a dataset of 24K trajectories by computing pick-and-place motions with random starting positions and environment configurations using a Rapidly exploring Random Tree (RRT) followed by a Gauss-Newton trajectory optimizer [25] algorithm that considers the full-arm kinematics and the 3D workspace. In the training phase,

we only consider the end-effector state (i.e., position and velocity).

Each sub-policy $\pi_g : \tilde{s}_t \mapsto a_g^R$ maps the state of the system and outputs an action towards the goal. The state \tilde{s}_t is a concatenation of robot and environment states consisting of: end-effector position $p_{gripper}$, vector components of current gripper rotation in z-axis

$$\mathbf{v}_{rotz} = [\cos \varphi, \sin \varphi]^T \quad (4)$$

obstacle position $p_{obstacle}$. In our experiment, we constrict our environment to a 2-dim plane over the workspace.

C. Predicting User Intent

In the experiments, we consider a simple intent inference model proposed in [6], based on distance and direction towards the goal.

The score b_g describes how likely the object is the goal object. Here, we use the posterior probability value for each object. The goal object g^* can be chosen as the object that maximizes the posterior probability given a history of observed features $\xi_{S \rightarrow U}$ [6], [23].

$$g^* = \arg \max_{g \in \mathcal{G}} P(g | \xi_{S \rightarrow U}) \quad (5)$$

We follow Dragan and Srinivasa [6] to compute $P(g | \xi_{S \rightarrow U})$ by using sum of squared velocity magnitudes as the cost function.

D. Simulating Human Users

In the experiments, we simulate human policies to replace the interaction with the reinforcement learning agent during training and evaluation:

- *Noisy* user as a sub-optimal noisy policy
- *Straight* user executes a policy that points directly to the goal
- *Biased* user misperceives the goal location due to imprecise perception (e.g. perceiving the goal closer than it actually is)

Both *Noisy* and *Biased* users make use of the policy described in Section IV-B. The *Noisy* user adds random noise at each time step to the policy, whereas the *Biased* user adds a random offset to the goal position.

E. Training Details

The DDPG arbitration module takes as input a 17-dimensional s_t including user action, all sub-policies and scores, and environment states (distance to goals, gripper position, and distance to the obstacle). s_t excluding the user action is passed through three dense layers of 32 units followed by a layer of two units. We refer to this part of the network as the “head”. The head is concatenated with the user action and passed through three dense layers of 16 units and outputs a continuous two-dimensional action, which represents the arbitrated action. This is referred to as the actor network.

The critic network uses the same head structure. The user action and the arbitrated action are concatenated with the

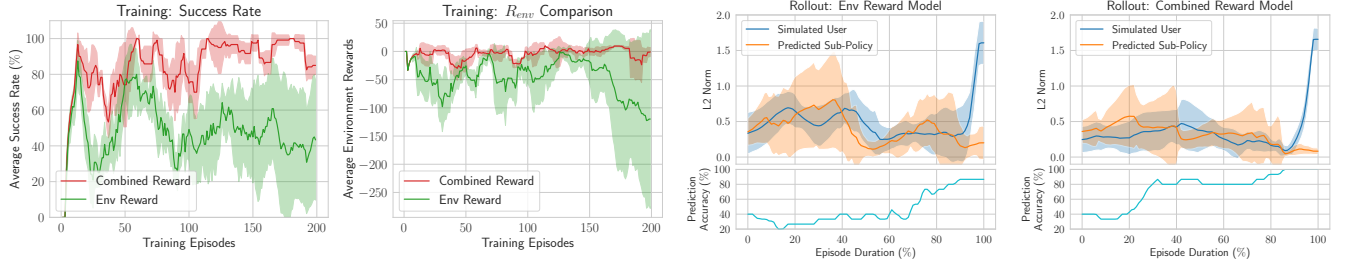


Fig. 3: (First two plots): Comparison between the policies with different reward functions during training, each averaged across 12 trained models and smoothed using a moving average (window size: 10 episodes).

(Last two plots): Demonstrations of the trained models, each averaged across 15 random setting episodes. The blue line indicates the L2 norm between the human action and the arbitrated action and the orange line indicates the L2 norm between the action from the sub-policy with the highest score (predicted sub-policy) and the arbitrated action.

output of the critic network’s head and connected to two dense layers of 128 units. The output of the critic network is a one-dimensional value that estimates the expected return after taking an action at a state.

The head is pretrained such that it learns to output the sub-policy with the highest score given all sub-policies, scores, and the environment information. This pretrained head is substituted in both actor, critic networks with frozen weights. The remaining layers of the arbitration module are also pretrained, such that the arbitration module eventually outputs the sub-policy with the highest score after the head network is concatenated with the user action. This way, the arbitration module is initialized to give full control to the robot and lowers its arbitration level as it interacts with the user.

This pretraining step was essential to lower the sample complexity of the algorithm. Without pretraining, the user must interact with random arbitrated actions which would make the user fight for control authority during training. In addition, the random trajectory that the robot creates from random arbitrated actions makes it even difficult to predict the goal and it exacerbates the training by generating noisy prediction scores.

V. RESULTS

A. Effects of Penalizing Disagreement during Training

We aim to see whether our reward function is beneficial during training and can lead to successfully learning an arbitration policy.

As shown in the first plot in Figure 3, the combined reward model ($R_{agree} + R_{env}$) converged to a high success rate ($> 90\%$) after 110 training episodes, whereas the success rate of the environment reward model (R_{env}) decreased over training. Taking into account that our goal prediction model is not perfect, we can assume that the combined reward model learned to assign more control authority to the user in the decision points where the FVMM is multimodal, rather than solely relying on the prediction and assisting towards the goal with the highest score.

When comparing the R_{env} term for both models (see Figure 3 second plot), the combined reward model outperformed the environment reward model by maintaining a stable R_{env} .

R_{env} is penalized at each time step when there is a collision with the obstacle or goes out of bounds and rewarded once it reaches the goal object. The combined reward model assured safer teleoperation by having fewer collisions and remaining inside the workspace boundary. It learned to avoid obstacles by allocating more control authority to the robot near the obstacle, where the FVMM is unimodal since all sub-policies agree by pointing outwards away from the obstacle.

B. Rolling Out the Trained Models

We demonstrated rollouts using the trained models to see how the arbitration policy behaves during an episode. We selected the trained models with the best return and demonstrated 15 randomized episodes. The *Straight* user mode was used as the human policy for the last two plots in Figure 3.

As desired, the combined reward policy flexibly allocates the control authority depending on the situation. In the beginning of the episode (duration $< 30\%$), the arbitrated policy was closer to the human policy. This is when the robot arm approaches the first decision point and should decide which way to get around the obstacle with low prediction accuracy. In the middle of the episode when the robot gripper must get around the obstacle (duration $40\% \sim 60\%$), the arbitrated policy is closer to the predicted sub-policy, which shows that the robot takes more control near the obstacle. Towards the end of the episode (duration $60\% \sim 80\%$) when the robot gripper encounters the second decision point to decide the goal object, the arbitrated policy is closer to the human policy, and the human gains more control authority. At the end of the episode, the arbitrated policy is closer to the predicted sub-policy, which provides more assistance when grabbing the object.

This effect was less prominent in the plot using the environment reward policy. In addition, the L2 norms for the environment reward were comparably higher than that of the combined reward in the first half of the episode. The arbitrated policy was neither close to both human and predicted sub-policy, meaning that the arbitrated policy generated policies that do not comply with both policies.

C. Comparison between Different Simulated Users

Table I shows the result of demonstrations from the learned policies for all user modes: *Noisy* user with two different noise sizes, *Straight* user, and *Biased* user. No assistance was applied in the direct control method.

Although the combined reward policy did not show the shortest travel distance among other assistance methods, it achieved more successful episodes and fewer collisions for all users than the environment reward policy. A compromise in the travel distance would have been necessary to avoid the obstacle from a safe distance. It is clearly shown from the *Straight* user that the combined reward policy had augmented the straight path to avoid the obstacle.

With the *Noisy* user, the combined reward policy showed a shorter travel distance than the direct control method, implying that the combined policy counterbalanced the noise. The combined reward policy was also beneficial for the *Biased* user, correcting the imprecise user commands to grab the goal object.

Overall results show that the R_{agree} term in the combined reward policy leads to successfully learning a policy that accurately assists towards the user's intended goal while maintaining safety.

TABLE I: Rollouts with simulated users over 15 episodes

User Mode	Assistance Method	Success	Travel Dist. (cm)	Collisions
Noisy 0.5	Combined Reward	14/15	53.68 \pm 3.17	0/15
	Environment Reward	12/15	53.06 \pm 2.64	2/15
	Direct Control	14/15	59.12 \pm 16.09	1/15
Noisy 1.0	Combined Reward	14/15	59.41 \pm 18.70	0/15
	Environment Reward	12/15	53.99 \pm 4.06	2/15
	Direct Control	14/15	71.16 \pm 13.23	0/15
Straight	Combined Reward	13/15	51.63 \pm 1.65	2/15
	Environment Reward	10/15	54.02 \pm 2.38	9/15
	Direct Control	11/15	49.19 \pm 2.17	7/15
Biased	Combined Reward	8/15	54.60 \pm 11.81	0/15
	Environment Reward	6/15	62.54 \pm 21.46	1/15
	Direct Control	3/15	65.27 \pm 22.21	0/15

VI. CONCLUSION

We proposed a framework to learn an arbitrated policy for shared control using DDPG that can dynamically hand over control authority to the user at a decision point. We identified the decision points by looking at the diversity of the sub-policies and constructing a Finite von Mises Mixture model to observe the modality of the distribution. Experiment results indicate that incorporating the implicit feedback allows the agent to effectively learn when to hand over control authority while maintaining safe and accurate teleoperation despite an imperfect goal prediction system. A limitation of our work is the lack of user interaction, which we will investigate as future work.

ACKNOWLEDGMENT

This work is partially funded by the research alliance ‘‘System Mensch’’. The authors thank the International Max

Planck Research School for Intelligent Systems (IMPRS-IS) for supporting Yoojin Oh.

REFERENCES

- [1] C. Phillips-Grafflin, *et al.*, ‘‘From autonomy to cooperative traded control of humanoid manipulation tasks with unreliable communication,’’ *Journal of Intelligent & Robotic Systems*, vol. 82, no. 3-4, pp. 341–361, 2016.
- [2] M. Johns, *et al.*, ‘‘Exploring shared control in automated driving,’’ *ACM/IEEE Int. Conf. on Human-Robot Interaction (HRI)*, 2016.
- [3] K. Muelling, *et al.*, ‘‘Autonomy infused teleoperation with application to brain computer interface controlled manipulation,’’ *Autonomous Robots*, vol. 41, no. 6, pp. 1401–1422, 2017.
- [4] A. Goil, *et al.*, ‘‘Using machine learning to blend human and robot controls for assisted wheelchair navigation,’’ in *2013 IEEE 13th International Conference on Rehabilitation Robotics (ICORR)*, 2013.
- [5] T. P. Lillicrap, *et al.*, ‘‘Continuous control with deep reinforcement learning,’’ *arXiv preprint arXiv:1509.02971*, 2015.
- [6] A. D. Dragan and S. S. Srinivasa, ‘‘A policy-blending formalism for shared control,’’ *The International Journal of Robotics Research*, vol. 32, no. 7, pp. 790–805, 2013.
- [7] A. A. Allaban, *et al.*, ‘‘A blended human-robot shared control framework to handle drift and latency,’’ *arXiv preprint arXiv:1811.09382*, 2018.
- [8] C. Schultz, *et al.*, ‘‘Goal-predictive robotic teleoperation from noisy sensors,’’ *IEEE Int. Conf. Robotics And Automation (ICRA)*, 2017.
- [9] D. Gopinath, *et al.*, ‘‘Human-in-the-loop optimization of shared autonomy in assistive robotics,’’ *IEEE Robotics and Automation Letters*, vol. 2, no. 1, pp. 247–254, 2016.
- [10] D.-J. Kim, *et al.*, ‘‘How autonomy impacts performance and satisfaction: Results from a study with spinal cord injured subjects using an assistive robot,’’ *IEEE Transactions on Systems, Man, and Cybernetics-Part A: Systems and Humans*, vol. 42, no. 1, pp. 2–14, 2011.
- [11] S. Javdani, *et al.*, ‘‘Shared autonomy via hindsight optimization for teleoperation and teaming,’’ *The International Journal of Robotics Research*, vol. 37, no. 7, pp. 717–742, 2018.
- [12] A. Broad, *et al.*, ‘‘Operation and imitation under safety-aware shared control,’’ in *Workshop on the Algorithmic Foundations of Robotics*, 2018.
- [13] —, ‘‘Highly parallelized data-driven mpc for minimal intervention shared control,’’ *Robotics: Science and Systems (RSS)*, 2019.
- [14] Y. Oh, *et al.*, ‘‘Natural gradient shared control,’’ *IEEE Int. Symp. on Robot and Human Interactive Communication (RO-MAN)*, 2020.
- [15] V. Mnih, *et al.*, ‘‘Human-level control through deep reinforcement learning,’’ *Nature*, vol. 518, no. 7540, pp. 529–533, 2015.
- [16] D. Silver, *et al.*, ‘‘Mastering the game of go with deep neural networks and tree search,’’ *Nature*, vol. 529, no. 7587, pp. 484–489, 2016.
- [17] W. Xu, *et al.*, ‘‘Reinforcement learning-based shared control for walking-aid robot and its experimental verification,’’ *Advanced Robotics*, vol. 29, no. 22, pp. 1463–1481, 2015.
- [18] J. Gao, *et al.*, ‘‘Xt2: Training an x-to-text typing interface with online learning from implicit feedback,’’ *International Conference on Learning Representations (ICLR)*, 2021.
- [19] S. Reddy, *et al.*, ‘‘Shared autonomy via deep reinforcement learning,’’ *arXiv preprint arXiv:1802.01744*, 2018.
- [20] C. Schaff and M. R. Walter, ‘‘Residual policy learning for shared autonomy,’’ *arXiv preprint arXiv:2004.05097*, 2020.
- [21] F. C. Fernandez and W. Caarls, ‘‘Deep reinforcement learning for haptic shared control in unknown tasks,’’ *arXiv preprint arXiv:2101.06227*, 2021.
- [22] Y. Du, *et al.*, ‘‘Ave: Assistance via empowerment,’’ *Neural Information Processing Systems (NeurIPS)*, 2020.
- [23] S. Jain and B. Argall, ‘‘Probabilistic human intent recognition for shared autonomy in assistive robotics,’’ *ACM Transactions on Human-Robot Interaction (THRI)*, vol. 9, no. 1, pp. 1–23, 2019.
- [24] E. Gumbel, *et al.*, ‘‘The circular normal distribution: Theory and tables,’’ *Journal of the American Statistical Association*, vol. 48, no. 261, pp. 131–152, 1953.
- [25] J. Mainprice, *et al.*, ‘‘Warping the workspace geometry with electric potentials for motion optimization of manipulation tasks,’’ *IEEE/RSJ Int. Conf. on Intel. Robots And Systems (IROS)*, 2016.